New kind of Hermite–Gaussian-like optical vortex generated by cross phase

Chen Wang (王 琛)[1], Yuan Ren (任 元)[1,2,*], Tong Liu (刘 通)[1], Linlin Chen (陈琳琳)[1], and Song Qiu (邱 松)[1]

[1]*Department of Aerospace Science and Technology, Space Engineering University, Beijing 101416, China*
[2]*State Key Laboratory of Laser Propulsion & Application, Space Engineering University, Beijing 101416, China*
**Corresponding author: renyuan_823@aliyun.com*

Received June 1, 2020; accepted June 16, 2020; posted online August 7, 2020

We propose a new kind of optical vortex called the Hermite–Gaussian-like optical vortex (HGOV) inspired by the cross phase (CP). Theoretically, we investigate how the CP is decoupled from the phase of a cylindrical lens. We also investigate the propagation characteristics of an HGOV, which has a Hermite–Gaussian-like intensity distribution but still retains the orbital angular momentum. Furthermore, we derive the Fresnel diffraction integral of an HGOV and study the purity at infinity. Besides, we show a novel function of the self-measurement of the HGOV. Finally, we show that we can change the relative positions of singularities and the direction of an HGOV precisely, which facilitates applications in optical micro-manipulation.

Keywords: Hermite-Gaussian-like optical vortex; cross-phase; orbital angular momentum.
doi: 10.3788/COL202018.100501.

Optical vortices (OVs) with the phase factor $\exp(im\varphi)$ carry orbital angular momentum (OAM) of $m\hbar$ per photon, where m denotes the topological charge (TC), φ denotes the azimuthal angle, and $\hbar$ is the Planck constant. Nowadays, OVs are motivating a plethora of applications[1,2], such as optical micro-manipulation[3,4], optical communication[5,6], high-dimensional quantum entanglement[7], and remote sensing of the angular rotation of structured objects via the optical rotation Doppler effect[8,9].

In 2019, the cross phase (CP), a new kind of phase structure, has been involved in Laguerre–Gauss (LG) beams that open up a new horizon for generation and measurement of OVs[10,11]. Recently, we investigated a generation and measurement method of high-order OVs via the CP, which has been experimentally achieved[12]. However, we ignored the OAM spectrum and only judged the generated beams by their intensity and phase distributions in Ref. [12]. Lately, we find that the OVs modulated by the CP are not the strictly Hermite–Gaussian (HG) mode due to the abnormal OAM spectrum.

In this Letter, inspired by the finding above, we propose a new kind of OV called the Hermite–Gaussian-like OV (HGOV), which has an HG-like intensity distribution but still retains the OAM. HGOVs have a novel function of the self-measurement, which reveals the value and sign of TCs. Further, HGOVs effectively decouple the phase of a spherical lens from the phase of a cylindrical lens, which allows us to control the HGOV more flexibly, whether at near-field or far-field. HGOVs also have a good depth of field due to relatively stable distributions at far-field, which has a significant meaning for precise three-dimensional (3D) optical tweezers. In addition, there have been many reports about the generation of multi-singular beams[13,14], but lots of them are based on the astigmatic mode converter, which has high requirements on the accuracy, such as the relative position of the cylindrical lenses and oblique incidence angle. Consequently, it is almost impossible to alter the positions of singularities precisely with the methods mentioned above. In contrast, HGOVs are more conducive to the precise manipulation of multi-particle and greatly evade the harsh requirements of the astigmatic mode converter with the help of a spatial light modulator (SLM), which is of great value in the field of multi-particle manipulation.

The form of the CP ψ in Cartesian coordinates (x, y) is

$$\psi(x,y)=u(x\cos\theta-y\sin\theta)(x\sin\theta+y\cos\theta),\tag{1}$$

where the coefficient u controls the conversion rate, and the azimuth factor θ characterizes the rotation angle of converted beams in one certain plane. It is noteworthy that Eq. (1) could be simplified to $\psi'(x,y)=uxy$ when $\theta=0$. The phase term of a cylindrical lens can be expressed as Eq. (2) when settled vertically:

$$\psi_p^{90^\circ}=\exp\left(ix^2\frac{k}{2f}\right),\tag{2}$$

which can be expanded into

$$\begin{aligned}\psi_p^{90^\circ}&=\exp\left\{\frac{ik}{2f}\left[\frac{1}{2}(x^2+y^2)+\frac{1}{2}(x^2-y^2)\right]\right\}\\&=\exp\left[\frac{ik}{2f}\frac{1}{2}(x^2+y^2)\right]\\&\quad\times\exp\left[\frac{ik}{2f}\left(\frac{\sqrt{2}}{2}x-\frac{\sqrt{2}}{2}y\right)\left(\frac{\sqrt{2}}{2}x+\frac{\sqrt{2}}{2}y\right)\right],\end{aligned}\tag{3}$$

where $k=2\pi/\lambda$, f denotes the focal length, and λ denotes the wavelength of the incident light. The term $(x^2+y^2)/2$

 © 2020 Chinese Optics Letters

is considered a spherical lens, and, if we take Eq. (1) into consideration, we can get

$$\psi_p^{90^\circ} = \exp\left[\frac{ik}{2f}\frac{1}{2}(x^2+y^2)\right] \times \exp\left[\frac{ik}{2f}\left(x\cos\frac{\pi}{4} - y\sin\frac{\pi}{4}\right)\left(x\sin\frac{\pi}{4} + y\cos\frac{\pi}{4}\right)\right]. \quad (4)$$

Namely, a vertically placed cylindrical lens can be equivalent to one spherical lens plus one CP that is rotated by 45°. It is to be noted that the phase of a spherical lens limits the generated beams to shape in the back focal plane (or at the far-field), but utilizing the CP to generate HGOVs effectively decouples the phase of a spherical lens from the phase of a cylindrical lens. It allows us to control the HGOV more flexibly, whether at the near-field or far-field. Decoupling the spherical lens has the following advantages. Firstly, we can use the rotation of the HGOV during the propagation to achieve a curved path for particle 3D manipulation. Secondly, if we need a focused HGOV, we can load the phase of a spherical lens with any focal length by an SLM, which is not limited by the fixed focal length of the cylindrical lens. Further, HGOVs have a good depth of field due to relatively stable distributions at the far-field, which has a significant meaning for precise control of 3D optical tweezers. Besides, due to the split singularities, HGOVs possess a unique advantage that could manipulate multiple particles precisely and dynamically at the same time. It is noteworthy that we define the light field that meets the far-field condition as the far-field hereinafter.

In fact, the coefficient u in a CP needs to be adjusted to meet the requirements for different initial conditions, which is similar to the cylindrical lens that has the following requirement for the waist radius ω of the incident light[15]:

$$\omega = \sqrt{\frac{(1+\sqrt{2})f\lambda}{\sqrt{2}\pi}}. \quad (5)$$

Thus, if $k/(2f)$ is set to u, we can derive the expression of u as

$$u = \frac{1+1/\sqrt{2}}{\omega^2}. \quad (6)$$

Without loss of generality, may the form of HGOV with $m = 1$ be

$$U(x,y,0) = \exp\left(-\frac{x^2+y^2}{\omega^2}\right)\exp(x-iy)\psi'(x,y). \quad (7)$$

According to the Fresnel diffraction integral, when the light field mentioned above propagates a certain distance z, the output can be expressed as

$$E(x,y,z) = \frac{1}{i\lambda z}\exp(ikz)\exp\left[\frac{ik}{2z}(x^2+y^2)\right] \times \mathcal{F}\left\{U(x_0,y_0,0)\exp\left[\frac{ik}{2z}({x_0}^2+{y_0}^2)\right]\right\}, \quad (8)$$

where (x,y,z) denotes the observation plane, and $\mathcal{F}$ is the Fourier transform.

Firstly, we would like to introduce the propagation properties of an HGOV from the near-field to the far-field. Under the condition of the coefficient $\omega = 1\,\text{mm}$, we simulate the propagation of the HGOV from 0 m to 5 m, as shown in Fig. 1. As the propagation distance increases, intensity distributions of the HGOV gradually tend to HG distributions. However, phase distributions of the HGOV gradually tend to distributions of an OV. Furthermore, to confirm the specific situation of the phase distributions, we also calculate the OAM spectra. The OAM spectrum for an arbitrary field Ψ can be calculated with[16,17]

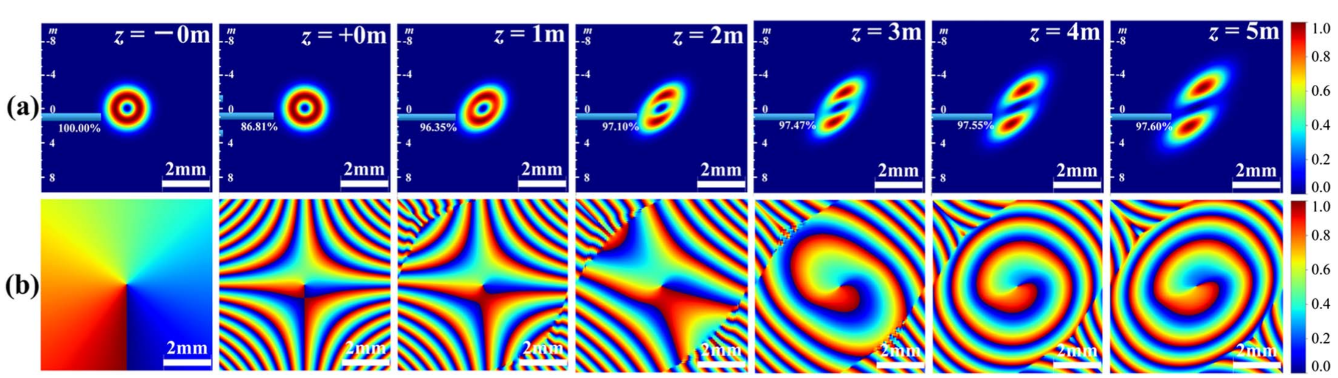

Fig. 1. Simulated propagation of the HGOV from 0 m to 5 m. $z = -0\,\text{m}$ denotes the original OV with no CP at 0 m, and $z = +0\,\text{m}$ denotes the OV immediately with the CP. (a) Simulated intensity distributions of the HGOV, where blue histograms denote the OAM spectra, and the percentage marked in the figures represents the proportion of $m = 1$. (b) Simulated phase distributions corresponding to (a).

$$P_m = \frac{C_m}{\sum_{-\infty}^{+\infty} C_n}, \tag{9}$$

where

$$C_m = \int_0^{\infty} \langle a_m(r,\varphi,z) \cdot |a_m(r,\varphi,z)\rangle r\mathrm{d}r, \tag{10}$$

$$a_m(r,z) = 1/(2\pi)^{1/2}\int_0^{2\pi} \Psi(r,\varphi,z)\exp(-im\varphi)\mathrm{d}\varphi, \tag{11}$$

and (r,φ,z) denotes the polar coordinate thereof. For simplicity and without loss of generality, the parameter n ranges from -8 to $+8$. The calculated OAM spectra are shown in Fig. 1(a), and the percentage marked in the figures represents the proportion of $m = 1$. The increasing mode purity of HGOVs also confirms the fact that the phase gradually changes to the phase of the OV of $m = 1$, which means the CP only changes the intensity distributions but keeps the most OAM, especially when the HGOV propagates to the far-field. Unfortunately, even if an HGOV propagates to the far-field, the purity still cannot reach 100% according to our simulated results. However, HGOVs have a good depth of field due to relatively stable distributions at the far-field, which has a significant meaning for precise 3D optical tweezers.

Secondly, we would like to generalize the situation of the HGOV from the far-field to infinity to figure out if there is any possibility that the HGOV can reach the 100% mode purity. Figure 1 is the numerical simulation based on Eqs. (7) and (8). In this part, we would like to derive the analytical expressions for the Fresnel diffraction integral after substituting Eq. (7) into Eq. (8):

$$\begin{aligned} E(x,y,z) &= \frac{1}{i\lambda z}\exp(ikz)\exp\left[\frac{ik}{2z}(x^2+y^2)\right] \\ &\times \mathcal{F}\left[\exp\left(-\frac{x_0^2+y_0^2}{\omega^2}\right)(x_0 - iy_0)\right] \\ &* \mathcal{F}\left\{ux_0y_0\exp\left[\frac{ik}{2z}(x_0^2+y_0^2)\right]\right\}, \end{aligned} \tag{12}$$

where $*$ denotes the convolution. Using Eq. (13), we can simplify Eq. (12) to Eq. (14):

$$\begin{aligned} &\int_{-\infty}^{\infty} x^n \exp(-px^2 + 2qx)\mathrm{d}x \\ &= n!\exp\left(\frac{q^2}{p}\right)\sqrt{\frac{\pi}{p}}\left(\frac{q}{p}\right)^n \sum_{s=0}^{[\frac{n}{2}]}\frac{1}{(n-2s)!s!}\left(\frac{p}{4q^2}\right)^s \\ &= \sqrt{\frac{\pi}{p}}\exp\left(\frac{q^2}{p}\right)\sum_{s=0}^{[\frac{n}{2}]}\frac{n!}{(n-2s)!s!}p^{s-n}4^{-s}q^{n-2s}, \end{aligned} \tag{13}$$

$$\begin{aligned} E(x,y,z) &= \frac{\pi}{2\lambda z^2(\beta\alpha)^{3/2}}(-kx\alpha + U\gamma_1 z) \\ &\times \exp\left(ikz + ik\frac{x^2+y^2}{2z} + \frac{\gamma_1^2}{\alpha} - \frac{k^2x^2}{4\beta z^2}\right) \\ &+ i\frac{\pi}{2\lambda z^2(\beta\alpha)^{3/2}}(ky\alpha - U\gamma_2 z) \\ &\times \exp\left(ikz + ik\frac{x^2+y^2}{2z} + \frac{\gamma_2^2}{\alpha} - \frac{k^2y^2}{4\beta z^2}\right), \end{aligned} \tag{14}$$

where

$$\begin{cases} \alpha = \frac{1}{\omega^2} + k\frac{1}{2iz} + \frac{U^2}{4\beta} \\ \beta = \frac{1}{\omega^2} + k\frac{1}{2iz} \\ \gamma_1 = \frac{1}{2}(k\frac{y}{iz} + k\frac{xU}{2\beta z}) \\ \gamma_2 = \frac{1}{2}(k\frac{x}{iz} + k\frac{yU}{2\beta z}) \end{cases}. \tag{15}$$

When $z \to +\infty$, $E(x,y,+\infty) \propto (-x + iy)$, which means that we only get a pure HGOV at infinity. Interestingly, due to decoupling the phase of a spherical lens from the phase of a cylindrical lens, we maintain the consistency of OAM growth rather than decreasing even when flipping the sign of OAM[18,19]. In Ref. [19], based on the ABCD matrix theory, the total OAM at the initial plane is

$$\Lambda(0) = \frac{\Phi}{c^2k}m, \tag{16}$$

where Φ is the total energy flux carried by the beam, and c is the light velocity. The OAM after the cylindrical lens is

$$\Lambda(z) = \frac{\Phi m}{c^2k}\frac{(\frac{z}{z_R})^2 + (1 - \frac{z}{f_x})}{(\frac{z}{z_R})^2 + \frac{1}{2}(1-\frac{z}{f_x})^2 + \frac{1}{2}}, \tag{17}$$

where $z_R = 4k\omega^2$, and f_x denotes the focal length of the cylindrical lens. Although the CP is part of the phase of a cylindrical lens, we can think that the phase of the spherical lens in Eq. (3) is close to a plane at infinity. Namely, within the condition that the propagation distance is infinity, we can calculate the OAM of the HGOV by Eq. (17), when $z \to +\infty$, $\Lambda(z) \to \Phi m/c^2k$, which is exactly equal to the OAM at the initial plane. This conclusion confirms the OAM distribution of an HGOV at infinity from the perspective of energy flow.

Nevertheless, HGOVs can still maintain high-mode purity at the far-field. Furthermore, HGOVs keep the OAM of an OV while retaining the function of the self-measurement, as shown in Fig. 2. We can directly get the TCs of the HGOVs, which are 2, 3, 4, and 5, respectively. Meanwhile, the mode purity of simulated HGOVs remains above 97%. We know from phase distributions of Fig. 2(b) that singularities of HGOVs have been split. However, we are only concerned with the total OAM distributions of an HGOV. Besides, due to the split singularities, the HGOV possesses a unique advantage that could

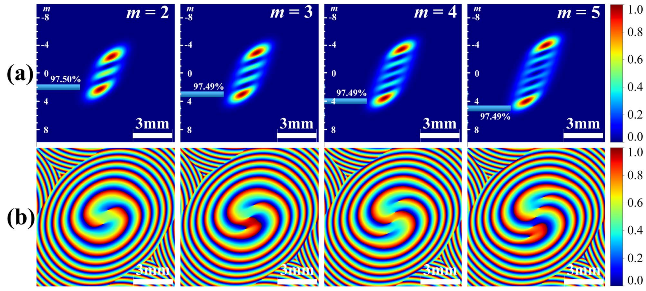

Fig. 2. Function of the self-measurement of the HGOV at the far-field. (a) Simulated intensity distributions of the HGOV of $m = 2$, 3, 4, and 5, respectively, where blue histograms denote the OAM spectra, and the percentage marked in the figures represents the proportion of $m = 2$, 3, 4, and 5, respectively. (b) Simulated phase distributions corresponding to (a).

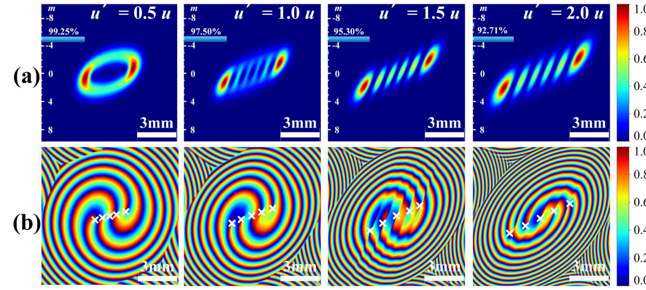

Fig. 4. Simulated distributions of HGOVs with different u': $u' = 0.5u$, $1.0u$, $1.5u$, and $2.0u$, respectively. (a) Simulated intensity distributions, where blue histograms denote the OAM spectra, and the percentage marked in the figures represents the proportion of $m = -5$. (b) Simulated phase distributions corresponding to (a), where the white crosses mark the locations of the singularities.

manipulate multiple particles precisely and dynamically at the same time, and we discuss this in detail below.

We can also use the function of the self-measurement to achieve the self-sign-measurement of the HGOV, as shown in Fig. 3. Generated HGOVs have different distributions when the TCs have the same value but an opposite sign at the far-field.

We would like to discuss the influence of the coefficient u on the generation of HGOVs. The coefficient u controls the conversion rate of an HGOV to the intensity distribution of the HG beam. However, we find that the mode purity decreases from 99.25% to 92.71% as the coefficient u' increases from $0.5u$ to $2.0u$ at the far-field, as shown in Fig. 4. We mark the locations of the singularities with the white crosses, and the distance range between neighboring singularities is from 0.2 mm to 0.5 mm. It is to be noted that we can change the relative positions of singularities precisely by altering the parameter u, which is of great value in the field of multi-particle manipulation. Further, the singularities of HGOVs have been split into multiple singular points with $m = 1$, which limits the ability of manipulation, but we can make up for this defect by increasing the incident optical power. In fact, the increase of the TCs means the increase of the radius of OVs, and the particles orbit along the direction of the phase gradient of OVs, which limits the minimum distance in multi-particle manipulation.

However, it is not enough to change the relative positions of singularities. We also need to accurately control the direction of an HGOV if we want to achieve multi-particle manipulation at any position. We know that the azimuth factor θ characterizes the rotation angle of an HGOV in one certain plane in Eq. (1), which makes it possible to achieve multi-particle manipulation anywhere. By altering the azimuth factor θ, we simulate HGOVs at 0°, 45°, 90°, and 135°, respectively, as shown in Fig. 5.

In summary, we propose a new kind of OV called the HGOV. Firstly, we show how the CP is decoupled from the phase of a cylindrical lens, which allows us to control the HGOV more flexibly, whether at the near-field or far-field. Secondly, we investigate the propagation

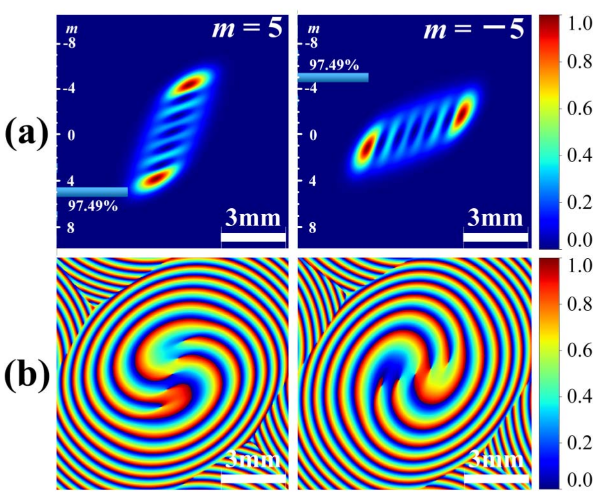

Fig. 3. Self-sign-measurement of the HGOV. (a) Simulated intensity distributions of the HGOV of $m = 5$, -5, where blue histograms denote the OAM spectra, and the percentage marked in the figures represents the proportion. (b) Simulated phase distributions corresponding to (a).

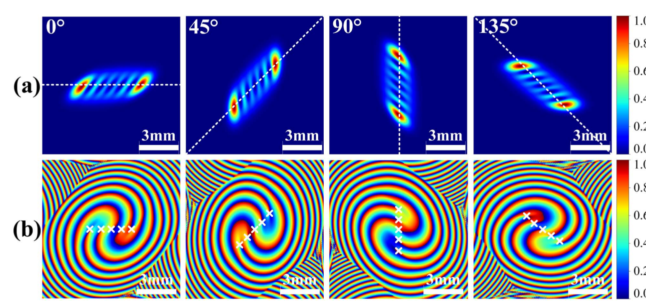

Fig. 5. Simulated results of HGOVs of $m = 5$ at 0°, 45°, 90°, and 135°, respectively. (a) Simulated intensity distributions. The white dotted lines are the axis of symmetry of HGOVs. (b) Simulated phase distributions corresponding to (a), where the white crosses mark the locations of the singularities.

characteristics of HGOVs, which have an HG-like intensity distribution but still retains the OAM at the far-field. HGOVs have a good depth of field due to relatively stable distributions at the far-field, which has a significant meaning for precise control of 3D optical tweezers. Theoretically, we derived the diffraction integral formula of HGOVs, which confirms that pure HGOVs only exist at infinity. We also confirm this conclusion from the perspective of energy flow. Thirdly, we introduce a novel function of HGOVs that the function of the self-measurement, which reveals the value and sign of TCs, no longer needs interferometry to measure it. Further, we discuss the influence of the coefficient u on the generation of HGOVs and find that the mode purity decreases as the coefficient u increases at the far-field. In addition, we show that we can change the relative positions of singularities and the direction of HGOVs precisely, which is of great value in the field of multi-particle manipulation.

This work was supported in part by the National Natural Science Foundation of China (Nos. 11772001 and 61805283), the Key Basic Research Projects of the Foundation Strengthening Plan (No. 2019-JCJQ-XX-XXX), and the Fund of State Key Laboratory of Laser Propulsion & Application (Nos. SKLLPA-04 and SKLLPA-05).

References

1. P. Chen, L. L. Ma, W. Duan, J. Chen, S. J. Ge, Z. H. Zhu, M. J. Tang, R. Xu, W. Gao, T. Li, W. Hu, and Y. Q. Lu, Adv. Mater. **30**, 1705865 (2018).
2. P. Chen, L. L. Ma, W. Hu, Z. X. Shen, H. K. Bisoyi, S. B. Wu, S. J. Ge, Q. Li, and Y. Q. Lu, Nat. Commun. **10**, 2518 (2019).
3. Y. Q. Zhang, X. Y. Zeng, L. Ma, R. R. Zhang, Z. J. Zhan, C. Chen, X. R. Ren, C. W. He, C. X. Liu, and C. F. Cheng, Adv. Opt. Mater. **7**, 9 (2019).
4. J. Wang, Chin. Opt. Lett. **16**, 050006 (2018).
5. G. Cossu, Chin. Opt. Lett. **17**, 100009 (2019).
6. X. Yang, S. Wei, S. Kou, F. Yuan, and E. Cheng, Chin. Opt. Lett. **17** (2019).
7. Y. J. Shen, X. J. Wang, Z. W. Xie, C. J. Min, X. Fu, Q. Liu, M. L. Gong, and X. C. Yuan, Light-Sci. Appl. **8**, 29 (2019).
8. S. Qiu, T. Liu, Z. Li, C. Wang, Y. Ren, Q. Shao, and C. Xing, Appl. Opt. **58**, 2650 (2019).
9. W. Zhang, D. Zhang, X. Qiu, and L. Chen, Phys. Rev. A **100**, 043832 (2019).
10. G. Liang and Q. Wang, Opt. Express **27**, 10684 (2019).
11. D. Shen and D. Zhao, Opt. Lett. **44**, 2334 (2019).
12. C. Wang, Y. Ren, T. Liu, C. Luo, S. Qiu, Z. Li, and H. Wu, Appl. Opt. **59**, 4040 (2020).
13. Y. Shen, Y. Meng, X. Fu, and M. Gong, J. Opt. Soc. Am. A Opt. Image Sci. Vis. **36**, 578 (2019).
14. Y. Wang, Y. Chen, Y. Zhang, H. Chen, and S. Yu, J. Opt. **18**, 055001 (2016).
15. J. Zhou, W. Zhang, and L. Chen, Appl. Phys. Lett. **108**, 8185 (2016).
16. H. I. Sztul and R. R. Alfano, Opt. Express **16**, 9411 (2008).
17. L. Torner, J. Torres, and S. Carrasco, Opt. Express **13**, 873 (2005).
18. A. Y. Bekshaev, M. S. Soskin, and M. V. Vasnetsov, Opt. Commun. **241**, 237 (2004).
19. A. Y. Bekshaev, M. S. Soskin, and M. V. Vasnetsov, J. Opt. Soc. Am. A Opt. Image Sci. Vis. **20**, 1635 (2003).